PROCEEDINGS OF SCIENCE

Interpretation of multimessenger anomalies of galactic cosmic rays with spatially dependent propagation model

Yu-Hua Yao,[a,b,*] **Xu-Lin Dong,**[c,b] **Yi-Qing Guo**[b,d] **and Qiang Yuan**[e,f]

[a] *College of Physics, Chongqing University, No.55 Daxuecheng South Road, High-tech District, Chongqing, 401331, China*

[b] *Key Laboratory of Particle Astrophysics, Institute of High Energy Physics, Chinese Academy of Sciences, No.19 B Yuquan Road, Shijingshan District, Beijing, 100049, China*

[c] *College of Physics, Hebei Normal University, No.20 Road East 2nd Ring South, Shijiazhuang, 050024, Hebei, China*

[d] *College of Physics, University of Chinese Academy of Sciences, No.19 A Yuquan Road, Shijingshan District, Beijing, 100049, China*

[e] *Key Laboratory of Dark Matter and Space Astronomy, Purple Mountain Observatory, Chinese Academy of Sciences, Nanjing 210008, China*

[f] *Center for High Energy Physics, Peking University, Beijing 100871, China*

E-mail: yaoyh@cqu.edu.cn

Recent observations of cosmic rays have presented compelling evidence for the presence of a two-component spectra anomaly that is observed across all primary and secondary particles, as well as the connecting ratios within the galactic plane. In this study, we propose a syngenetic origin for this two-component phenomenon, suggesting that it originates from two diffuse regions. With this scenario, we demonstrate that all anomalies, with the exception of the positron spectrum, can be naturally reproduced. Specifically, the break-off in the electron spectrum at TeV energies can be understood as a transition process from a regime where diffusion dominates to one where energy cooling effects become prominent. Moreover, we find that extending the two-component spectra model to encompass the entire galactic plane enables us to recreate the ultra-high energy emissions detected by the ASγ experiment. Consequently, our work establishes a clear physical framework for understanding the formation of galactic cosmic rays. Notably, the high-energy cosmic rays primarily originate from recent accelerators and remain confined to nearby locations, while the low-energy cosmic rays predominantly originate from remote sources within the galactic sea. In other words, cosmic rays below 200 GV stem from the galactic sea, whereas those above 200 GV, including those located at the knee position, primarily originate from sources in close proximity to us.

38th International Cosmic Ray Conference (ICRC2023)
26 July - 3 August, 2023
Nagoya, Japan

*Speaker

PoS(ICRC2023)158

1. Introduction

Cosmic rays (CRs) have intrigued scientists since their discovery, and recent advancements in spectrum measurements through space-borne experiments have provided invaluable insights into their properties. The ATIC-2, CREAM, PAMELA, and AMS-02 experiments have shed light on novel phenomena, uncovering a fine structure of spectral hardening at a rigidity of approximately 200 GV [1–4]. The AMS-02 measurements further revealed that this hardening is observed at the same rigidity for each individual nucleus (review [5] and therein). Moreover, the $\bar{p}/p$ ratio exhibits an energy-independent distribution above 10 GeV, as demonstrated by the AMS-02 measurements [6]. Recent data from DAMPE has also brought exciting news, showing breaks at 200 GeV in both the B/C and B/O ratios [7]. Beside nuclei, the positron and electron has similar structure above 10 and 42 GeV, respectively [8, 9]. In addition, the total spectrum of positron and electron has break-off around TeV [10]. Furthermore, a fascinating observation is the hardening of diffuse γ-rays occurring at approximately 10 GeV in the inner and outer regions [11], which is possibly supported by the Tibet-ASγ measurements in the ultra-high energy range [12]. The emergence of common features and the exploration of their origins present an intriguing avenue for further investigation.

A remarkable characteristic observed in various multi-messenger observations is the presence of two-component structures, referred to as Comp-A and Comp-B for convenience, displaying distinct power-law indices in the low- and high-energy regimes, respectively. This phenomenon is particularly prominent for primary CR species, where the junction between Comp-A and Comp-B occurs around a rigidity of approximately 200 GV, with the exception of electrons due to their rapid energy cooling. Understanding the origin of this junction necessitates an investigation into the spectra of secondary particles, which are influenced by pp-collision and fragmentation interactions. In these processes, the junction points for secondary species are observed to be roughly around 10 GeV and 200 GeV. Remarkably, in fragmentation interactions, secondary nucleons, such as Li, Be, B, maintain the same energy as their parent C, N, O nucleons. On the other hand, secondary particles like $\bar{\mathrm{p}}, \mathrm{e}^{+}$, and γ inherit approximately 10% of the energy from their parent protons in pp-collision interactions. Consequently, the intersection of Comp-A and Comp-B, considered the origin of all secondary particles, is situated at the rigidity of 200 GV. It is therefore logical to investigate potential common causes underlying these multi-messenger findings.

In this work, we propose that the inner-and-outer two-region diffusive process is the common origin of spectra anomaly. In this physical scenario, We intend to duplicate all of those multi-messenger findings. More importantly, we hope to use this investigation to determine the source of galactic CRs that have been seen in the solar system.

2. Model & Methodology

It is widely acknowledged CRs are generated and accelerated in astrophysical entities such as supernova remnants. Once they escape from their source regions, they disperse through a diffusive process involving multiple deflections caused by magnetic irregularities and interactions with the interstellar medium. Recent advancements in the exploration of two-component spectra and the pulsar halo have contributed valuable insights into this field.

Building upon these newly observed phenomena, we employ the two-diffuse-region model in our study. We postulate that each pulsar possesses a halo, characterized by the slow diffusion of particles. Not only does the halo act as a barrier, preventing CRs from neighboring sources from entering this region, but it also serves as a confinement area for CRs within the source region. This prolonged confinement within the halo results from its slow diffusion properties [13]. The Comp-B component of CRs, which undergoes recent acceleration, largely retains the characteristics of the source injection spectrum. Its noteworthy feature is the hardening spectral index, observed exclusively in CRs within galactic disks. In contrast, CRs originating from distant sources are less likely to traverse the galactic disk directly, opting instead to join the outer halo. In this outer halo, CRs undergo a faster diffusion process, giving rise to a considerably softer spectrum. Some of these CRs eventually return to the cosmic disk and eventually reach Earth.

The ubiquity of this component across the galaxy underscores its universal nature. Consequently, the underlying physical basis for the observed two-component spectra becomes readily evident. Moreover, given that adjacent sources contribute significantly to the Comp-B segment of CRs, it is plausible that the CRs in the knee region also originate from these sources. Subsequently, we aim to further our understanding of the propagation process. The transport equation governing the propagation of CRs is given by:

$$\begin{aligned}\frac{\partial\psi(\vec{r},p,t)}{\partial t} &= Q(\vec{r},p,t)+\vec{\nabla}\cdot(D_{xx}\vec{\nabla}\psi-\vec{V}_c\psi)\\ &+\frac{\partial}{\partial p}\left[p^2D_{pp}\frac{\partial}{\partial p}\frac{\psi}{p^2}\right]\\ &-\frac{\partial}{\partial p}\left[\dot{p}\psi-\frac{p}{3}(\vec{\nabla}\cdot\vec{V}_c)\psi\right]\\ &-\frac{\psi}{\tau_f}-\frac{\psi}{\tau_r}\,,\end{aligned} \tag{1}$$

where $\psi(\vec{r},p,t)$ represents the density of CRs, $Q(\vec{r},p,t)$ describes the source distribution, $\vec{V}c$ denotes the convection velocity, Dxx represents the spatial diffusion coefficient, D_{pp} represents the momentum diffusion coefficient associated with the re-acceleration process, and $\dot{p}$, τ_f, and τ_r are the energy loss rate, fragmentation time scale, and radioactive decay time scale, respectively.

We consider the confinement of CRs within a cylindrical region during their travel. The diffusive halo encompassing the Galactic disk is symmetrically divided into two zones according to the spatial-dependent propagation (SDP) hypothesis, resulting in a variation of the diffusion coefficient. Specifically, CRs disperse more slowly in the inner halo surrounding the Galactic disk than in the outer halo. The parameterization of D_{xx} is given by:

$$D_{xx}(r,z,\mathcal{R})=D_0F(r,z)\beta^\eta\left(\frac{\mathcal{R}}{\mathcal{R}_0}\right)^{\delta_0F(r,z)}, \tag{2}$$

where $F(r,z)$ is defined as:

$$F(r,z)=\begin{cases}g(r,z)+[1-g(r,z)]\left(\frac{z}{\xi z_0}\right)^n, & |z|\le\xi z_0,\ 1,\\ |z|>\xi z_0,\end{cases} \tag{3}$$

with $g(r,z)=\frac{N_m}{1+f(r,z)}$.

The key parameters governing CR propagation and source injection are provided in Table 1 and Table 2, respectively. To solve the transport equation, we employ the numerical package DRAGON.

Table 1: Parameters of the SDP propagation model.

D_0 [cm^{-2} s^{-1}]	δ_0	N_m	ξ	n	v_A [km s^{-1}]	z_0 [kpc]
4.4	0.63	0.24	0.1	4.0	6	4.5

Table 2: Injection spectra parameters of different components.

	p	C	e^-
Q_0[m^{-2} sr^{-1} GeV^{-1}]	4.55×10^{-2}	9.70×10^{-5}	0.27
ν	2.45	2.32	2.82

3. Results

Using the methodology described earlier, we conducted model calculations to determine the spectra of protons, leptons, and the connecting bridge for the B/C and $\bar{p}/p$ ratios. Subsequently, we expanded our computations to encompass the entire galactic plane diffuse γ-rays.

Figure 1 presents a comparison of the observed proton spectrum with the predictions from our SDP model. It is evident that the model accurately reproduces the phenomenon of spectrum hardening. To account for the distribution of sources, we divided the region surrounding the sun into two zones based on the height of the inner halo: $r_s < 0.6$ kpc and $r_s > 0.6$ kpc. A particularly intriguing observation is the significant similarity between the contribution from distant sources ($r_s > 0.6$ kpc) and the Comp-A data. This portion of the cosmic ray spectrum experiences the effects of rapid diffusion in the galactic halo, primarily manifesting in the low-energy range.

In order to replicate the observed spectral break-off at 14 TeV, as reported by DAMPE [14], we introduce distinct energy break-off values for the regions $r_s < 0.6$ kpc. This energy break-off may potentially be attributed to the presence of a nearby source [15, 16]. Nonetheless, it is evident that the contribution originating from nearby sources ($r_s < 0.6$ kpc) closely resembles that of Comp-B, which is confined within a region of slower diffusion and does not extend into the galactic halo.

Figure 2 presents the computed ratios of B/C and $\bar{p}/p$, comparing with the observations. Similar to proton spectrum, Comp-A shows rapid decline and distributed in whole galaxy as sea of secondary particles. Comp-B is unique to the galactic disk and dominates at high energy.

Figure 3 presents the calculated spectra of positrons and the combined spectra of positrons and electrons. When considering the normal interstellar radiation field (ISRF), the calculated spectra fall below the observed values. However, upon reducing the ISRF to 30% of its standard intensity, the calculated spectra show a partial agreement with the observations.

Under the SDP model, it becomes evident that the so-called diffuse and source terms represent the contributions from p-p collisions with the ISM within the galactic cosmic ray sea and from freshly accelerated CRs confined to source regions, respectively. This conclusion is supported by similar findings for primary electrons, as demonstrated in the right panel of Figure 3. Furthermore,

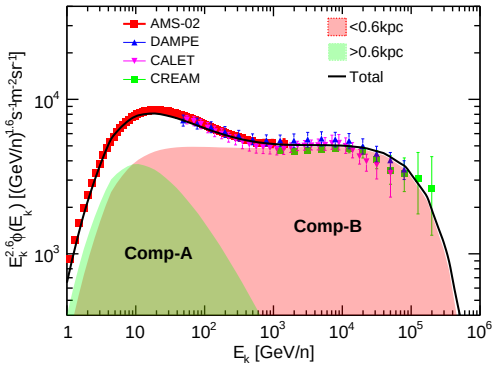

Figure 1: Proton spectrum model predictions compared to observations by AMS-02 [4], DAMPE [14] and CREAM-III [17]. The red, blue, and green dotted lines represent fluxes supplied by sources in the $r_s < 0.6$ kpc and $r_s > 0.6$ kpc regions, respectively. The innermost area uses 8×10^4 GeV as an energy break-off. The overall contribution is shown by the black solid line. The injection spectra are reported in Tab. 2, and the propagation parameters are listed in Tab. 1.

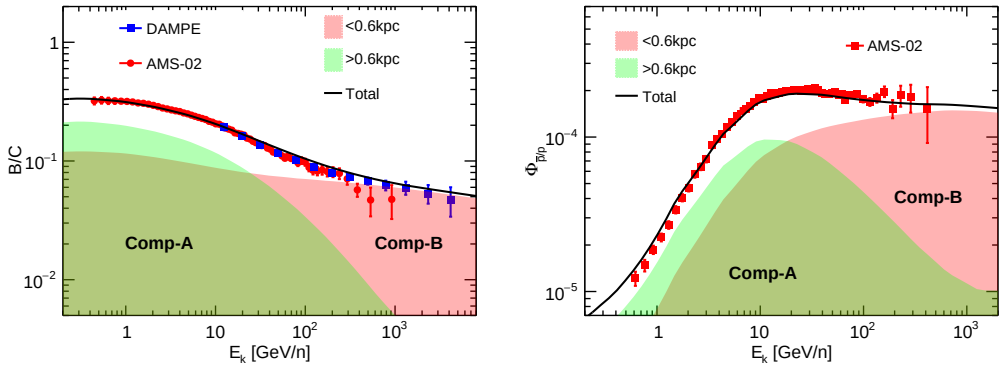

Figure 2: Model predictions of B/C (left) and $\bar{p}/p$ ratios (right) compared with the measurements of AMS-02 [6, 18] and DAMPE [7].

owing to the unique characteristics of the two diffuse regions, we successfully reproduce the spectral break-off at a critical TeV energy, which has been observed by DAMPE and H.E.S.S. [10, 20]. Of crucial importance is the transition from the dominance of the diffuse effects to the dominance of energy cooling effects. The presence of an electron spectral break-off further substantiates the existence of an inner halo.

The charge spectrum observed within the solar system provides support for the proposed physical explanation. Furthermore, the relationship between a two-component phenomenon and a two-diffuse region remains valid throughout the galactic plane. To further investigate this topic, the diffuse γ-rays serve as a valuable probe. Previous observations by Fermi-LAT have revealed a break-off in the spectrum of diffuse γ-rays at around 10 GeV (reference, 2010PhRvL.104j1101A). More recently, the ASγ experiment reported ultra-high-energy results, which necessitated an additional component contribution [12]. Figure 4 presents a comparison between the measured spectrum of

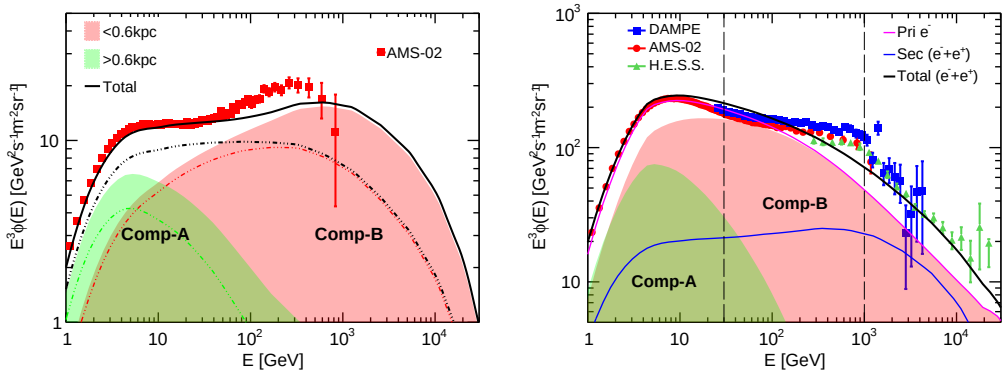

Figure 3: Left: positron flux from three different sources. The black lines represent total positron fluxes as measured by AMS-02 [9]. The red, blue, and green dot-dashed lines are the results of using the standard ISRF; the dotted lines with shadows are the fluxes when the ISRF is reduced to 30%. Right: The total of electron fluxes computed using parameters listed in Tab.2 and 1 using the standard ISRF, as well as positron fluxes under the ISRF weaken to 30%. Three energy zones, separated by two perpendicular lines, depict the dominating effect transit from particles' energy cooling effect to diffuse effect, and back to particles' energy cooling effect with rising energy. The data comes from AMS-02 [19], DAMPE [10] and H.E.S.S. [20].

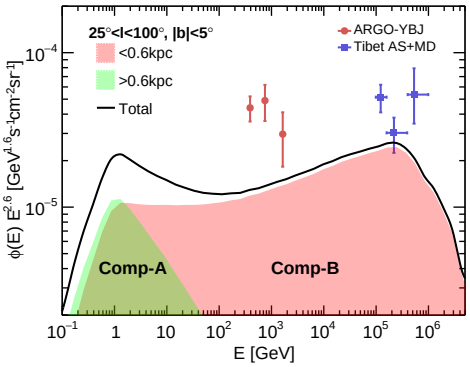

Figure 4: Flux of diffuse γ-ray emission in the regions of $|b| < 5°, 25° < l < 100°$, the data are from ARGO-YBJ [21] and ASγ experiments [12].

diffuse γ-rays and the estimated spectrum. Notably, it becomes apparent that the newly accelerated cosmic rays, referred to as Comp-B, can potentially account for an extra component of the diffuse γ-ray emissions.

4. Conclusions

The presence of the Geminga Halo, initially discovered by the HAWC collaboration, has been identified as a region characterized by significantly reduced dissemination [13]. Subsequent support for this finding was provided by the LHAASO experiment, which suggested the prevalence of halos surrounding pulsars [22]. Recent discoveries of additional pulsar halos further reinforce the notion

that a universal slow diffuse zone may exist within the galactic plane, encompassing all pulsars with slow diffuse halos.

In this study, our model calculations carefully consider the influence of the two diffuse regions of CRs. By incorporating these regions, we were able to successfully replicate the shared feature of the two-component structure observed in CR messengers. Through adjusting the energy cooling by approximately 30%, the excess spectra of positrons and electrons can be reasonably reconciled with observational data. The natural recreation of the spectral break-off occurring near the TeV range can be described as a transition from a diffuse-dominant to a cooling-dominant effect, owing to the distinctive characteristics of the two diffuse regions. Importantly, the origin of the two-component structures has been well-established. Comp-A enters the solar system from the outer halo and remains pervasive throughout our galaxy. Conversely, Comp-B represents newly accelerated particles constrained to a source region localized within the galactic plane. A significant finding of this study is that the majority of high-energy cosmic rays in the solar system, including those in the knee region, can be attributed to nearby sources.

References

[1] A. D. Panov, J. H. Adams, H. S. Ahn, et al. The results of ATIC-2 experiment for elemental spectra of cosmic rays. *arXiv e-prints*, pages astro–ph/0612377, December 2006.

[2] H. S. Ahn, P. Allison, M. G. Bagliesi, et al. Discrepant Hardening Observed in Cosmic-ray Elemental Spectra. ApJ, 714:L89–L93, May 2010.

[3] O. Adriani, G. C. Barbarino, G. A. Bazilevskaya, et al. PAMELA Measurements of Cosmic-Ray Proton and Helium Spectra. *Science*, 332:69–, April 2011.

[4] M. Aguilar, D. Aisa, B. Alpat, et al. Precision Measurement of the Proton Flux in Primary Cosmic Rays from Rigidity 1 GV to 1.8 TV with the Alpha Magnetic Spectrometer on the International Space Station. *Phys. Rev. Lett.*, 114(17):171103, May 2015.

[5] M. Aguilar, L. Ali Cavasonza, G. Ambrosi, et al. The Alpha Magnetic Spectrometer (AMS) on the international space station: Part II - Results from the first seven years. Phys. Rep., 894:1–116, February 2021.

[6] M. Aguilar, L. Ali Cavasonza, B. Alpat, et al. Antiproton Flux, Antiproton-to-Proton Flux Ratio, and Properties of Elementary Particle Fluxes in Primary Cosmic Rays Measured with the Alpha Magnetic Spectrometer on the International Space Station. *Phys. Rev. Lett.*, 117(9):091103, August 2016.

[7] DAMPE Collaboration. Detection of spectral hardenings in cosmic-ray boron-to-carbon and boron-to-oxygen flux ratios with dampe. *Science Bulletin*, 2022.

[8] M. Aguilar, D. Aisa, A. Alvino, et al. Electron and Positron Fluxes in Primary Cosmic Rays Measured with the Alpha Magnetic Spectrometer on the International Space Station. *Phys. Rev. Lett.*, 113(12):121102, September 2014.

[9] M. Aguilar, L. Ali Cavasonza, G. Ambrosi, et al. Towards Understanding the Origin of Cosmic-Ray Positrons. Phys. Rev. Lett., 122(4):041102, February 2019.

[10] DAMPE Collaboration, G. Ambrosi, Q. An, et al. Direct detection of a break in the teraelectronvolt cosmic-ray spectrum of electrons and positrons. Nature, 552(7683):63–66, December 2017.

[11] M. Ackermann, M. Ajello, W. B. Atwood, et al. Fermi-LAT Observations of the Diffuse γ-Ray Emission: Implications for Cosmic Rays and the Interstellar Medium. ApJ, 750:3, May 2012.

[12] M. Amenomori, Y. W. Bao, X. J. Bi, et al. First Detection of sub-PeV Diffuse Gamma Rays from the Galactic Disk: Evidence for Ubiquitous Galactic Cosmic Rays beyond PeV Energies. Phys. Rev. Lett., 126(14):141101, April 2021.

[13] A. U. Abeysekara, A. Albert, R. Alfaro, et al. Extended gamma-ray sources around pulsars constrain the origin of the positron flux at Earth. *Science*, 358:911–914, November 2017.

[14] Q. An, R. Asfandiyarov, P. Azzarello, et al. Measurement of the cosmic ray proton spectrum from 40 GeV to 100 TeV with the DAMPE satellite. *Science Advances*, 5(9):eaax3793, September 2019.

[15] Kun Fang, Xiao-Jun Bi, and Peng-Fei Yin. DAMPE Proton Spectrum Indicates a Slow-diffusion Zone in the nearby ISM. ApJ, 903(1):69, November 2020.

[16] Qiang Yuan, Bing-Qiang Qiao, Yi-Qing Guo, Yi-Zhong Fan, and Xiao-Jun Bi. Nearby source interpretation of differences among light and medium composition spectra in cosmic rays. *Frontiers of Physics*, 16(2):24501, October 2020.

[17] Y. S. Yoon, T. Anderson, A. Barrau, et al. Proton and Helium Spectra from the CREAM-III Flight. ApJ, 839:5, April 2017.

[18] M. Aguilar, L. Ali Cavasonza, G. Ambrosi, et al. Precision Measurement of the Boron to Carbon Flux Ratio in Cosmic Rays from 1.9 GV to 2.6 TV with the Alpha Magnetic Spectrometer on the International Space Station. Phys. Rev. Lett., 117(23):231102, Dec 2016.

[19] M. Aguilar, L. Ali Cavasonza, B. Alpat, et al. Towards Understanding the Origin of Cosmic-Ray Electrons. Phys. Rev. Lett., 122(10):101101, March 2019.

[20] D H.E.S.S. collaboration, Kerszberg, M Kraus, D Kolitzus, et al. The cosmic ray electron spectrum measured with h.e.s.s., 2017.

[21] B. Bartoli, P. Bernardini, X. J. Bi, et al. Study of the Diffuse Gamma-Ray Emission from the Galactic Plane with ARGO-YBJ. ApJ, 806(1):20, June 2015.

[22] F. Aharonian, Q. An, L. X. Axikegu, Bai, et al. Extended Very-High-Energy Gamma-Ray Emission Surrounding PSR J 0622 +3749 Observed by LHAASO-KM2A. Phys. Rev. Lett., 126(24):241103, June 2021.